ISSN (Print) : 0974-6846
ISSN (Online) : 0974-5645
Indian Journal of Science and Technology, *Vol 11(24), DOI: 10.17485/ijst/2018/v11i24/127418, June 2018*

Fault Tolerant Control of Electric Power Steering System with Sensor Fault

Allous Manel[1*] and Zanzouri Nadia[2]

[1]Laboratory (LACS) Analysis, Design and Control of Systems, National Engineering School of Tunis, Universite de Tunis El Manar, LR 11ES20LACS, Box 37, Le Belvedere 1002 Tunis, Tunisia; allousmanel@yahoo.fr

[2]Preparatory Engineering Institute of Tunis, Universite de Tunis, 2 RueJawaharlal Nehru Montfleury, 1089 Tunis, Tunisia; Nadia.Zanzouri@enit.rnu.tn

Abstract

Objectives: A novel approach for diagnosis and control design that compensates sensor fault effects in electric power steering system (EPS) is proposed. **Methods/Statistical Analysis:** A Luenberger observer is used to estimate the fault of torque sensor for the EPS system. The fault tolerant control (FTC) based an inverse model of bond graph (BG) is used to compensate the fault of torsion bar sensor signal. The proposed control strategy presents an opportunity to improve EPS system performance and also reduce system complexity. **Findings:** The findings achieved are simulation tests, showed that the application of the synthesized law on the experimental of the EPS system show the effectiveness of the proposed approach. **Application:** The fault tolerant control based a bond graph model is an important step allows an improvement the rapidity of the compensation of fault in the system.

Keywords: Bond Graph, Diagnosis, Fault Tolerant Control, Inverse Bond Graph

1. Introduction

In recent years, the electric power steering (EPS) system has been widely used as the automobile power-steering equipment because of its efficiency, modularity, and tenability. EPS is a control system that electrically amplifies the driver steering torque inputs to the vehicle to improve steering comfort and performance[1].

The steering system is an essential part of a vehicle, because not only does it steer the vehicle but it also conveys information about the road and vehicle to the driver. Automobile manufacturers introduced power steering systems to reduce the physical effort of drivers. EPS systems compared to HPS systems offer lower energy consumption, lower total weight and package exibility, at no cost penalty. In addition, with the increase of fuel prices, the fuel saving benefits of EPS systems make these products more economical than HPS systems.

Electric Power steering makes use of a torsion bar torque sensor to measure the torque of the driver. The EPS controller uses the torque sensor and the vehicle speed signal to determine the torque of assist motor. EPS controller sends a command signal to the motor controller to control the assist motor torque. Through a gearbox, the assist motor transfers the torque to the steering rack then to pinion. The power steering turns to manual steering, as no assist is provided, thus requiring the driver to provide the entire steering torque. This is an undesirable situation. To improve the reliability of the EPS system, a suitable fault management system needs to be implemented. For faults such as sensor fault, FTC may be implemented so as to give reasonably good performance. It is seen that most methods used in fault management systems apply a threshold to the residual to detect the presence of a fault[2] for this approach it used a model based Fault Detection and Isolation (FDI) technique. A fault tolerant control system for strain gauge sensor fault is discussed[3]. They are two methods for sensor less estimation, one considering disturbance torque as unknown input and the second one considering it as a state variable[4]. Different estimation schemes can be used to estimate the same signal quantities. The FTC control scheme is designed for a speed sensor fault in a DC motor drive

*Author for correspondence

system using sliding mode observers[5]. The same is accomplished using H2/H∞ techniques[6]. A detailed comparison between sliding mode, classical, and nonlinear extended Luenberger and Kalman observers for FDI[7].

This paper focuses on the problem of compensation of fault when takes place in the torque sensor. A Luenberger observer is used to estimate the sensor fault and FTC approach is used to compensate this fault in the system. This paper is organized in 5 sections where Section 2 gives the introduction of EPS system and describes the modeling of EPS with Bond Graph. Section 3 explains the fault tolerant control approach is based to the inverse bond graph model. In Section 4 the simulations results are presented and analyses and ended with conclusion and future work recommendation in Section 5.

2. EPS System Model

Electronic power steering (EPS) used the electric motor to assist the driver of a vehicle. This gives more assistance as the vehicle slows down, and less at faster speeds. An EPS system typically consists of a vehicle speed sensor, motor, a steering angle sensor, and Electronic Control Unit (ECU) as shown in Figure 1.

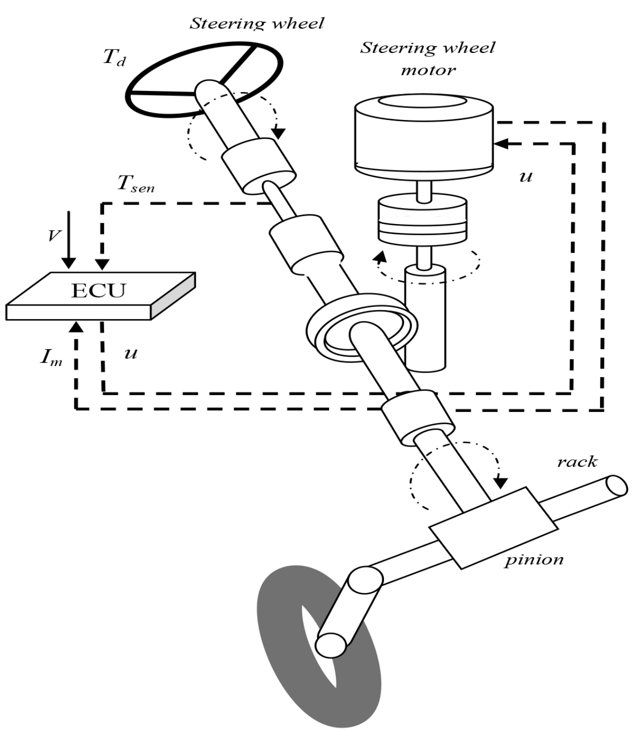

Figure 1. Structure of EPS system.

With T_d is the torque exerted by driver to control the vehicle direction, T_{sen} is the torsion bar sensor, I_m is the current of DC motor, V is the vehicle speed and u is the control in put of DC motor.

2.1 Modeling of EPS based a BG Model

The bond graph modeling is proposed by[8]. This tool allows that the multi domains systems (mechanical, electrical, thermal, etc.). The BG is more and more used for modeling and fault diagnosis. The first BG for the design of Luenberger observers has been developed by Karnopp for a control purpose[9]. The causal properties of the BG were initially used for the determination of the state estimation, diagnosis and simulation of dynamical systems. Bond-graph theory could be applied to EPS which is a controllable system with coupling of machine and electricity[10].

The bond graph model of EPS system is presented in Figure 2 and the elements considered in third figure are defined in Table 1.

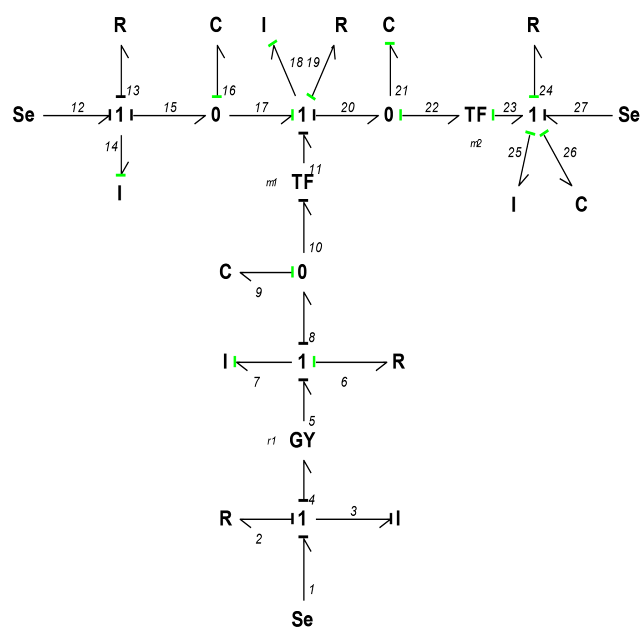

Figure 2. Bond graphs model of EPS.

Table 1. Steering wheel subsystem elements

Variable	Symbols used in the bond graph model
u	Se_1
R	R_2
L	I_3
K_b	r_1

B_m	R_6
J_m	I_7
K_m^{-1}	C_9
GY	m_1
T_d	Se_{12}
J	I_{14}
B	R_{13}
K_s^{-1}	C
J_e	I_1
B_e	R
K_e^{-1}	C
r_p	m_2
b_r	R_{24}
m_r	I_2
K_r^{-1}	C_{26}
F_δ	Se_{27}

The state equations of the EPS system are established using the bond graph method in FigureA DC electric motor is used in EPS systems to provide the assist torque[11]. The differential equations of motor are deduced as the following:

$$\dot{p}_3 = Se_1 - \frac{R_2}{I_3} p_3 - \frac{r_1}{I_7} p_7 \tag{1}$$

$$\dot{p}_7 = \frac{r_1}{I_3} p_3 - \frac{R_6}{I_7} p_7 - \frac{1}{C_9} q_3 \tag{2}$$

$$\dot{q}_9 = \frac{p_7}{I_7} - \frac{1}{m_1 I_{18}} p_{18} \tag{3}$$

The differential equations of steering system are deduced as the following:

$$\dot{p}_{14} = Se_{12} - \frac{R_{13}}{I_{14}} p_{13} - \frac{1}{C_{16}} q_{16} \tag{4}$$

$$\dot{q}_{16} = \frac{I}{I_{14}} p_{13} - \frac{1}{I_{18}} p_{18} \tag{5}$$

$$\dot{p}_{18} = \frac{1}{m_1 C_9} q_9 + \frac{1}{C_{16}} q_{16} - \frac{R_{19}}{I_{18}} p_{18} - \frac{1}{C_{21}} q_{21} \tag{6}$$

$$\dot{q}_{21} = \frac{p_{18}}{I_{18}} - \frac{1}{m_2 I_{25}} p_{25} \tag{7}$$

$$\dot{p}_{25} = \frac{1}{m_2 C_{21}} q_{21} - \frac{R_{24}}{I_{25}} p_{25} - \frac{1}{C_{26}} q_{26} + Se_{27} \tag{8}$$

$$\dot{q}_{26} = \frac{1}{I_{25}} p_{25} \tag{9}$$

The linear EPS system can be expressed in the state space form:

$$\begin{cases} \dot{x}(t) = Ax(t) + Bu_{EPS}(t) \\ y(t) = Cx(t) \end{cases} \tag{10}$$

where the state vector model is:

$$x = \begin{bmatrix} p_3 & p_7 & q_9 & p_{14} & q_{16} & p_{18} & q_{21} & p_{25} & q_{26} \end{bmatrix}^T$$

The control input u of DC motor, the driver torque and the random road force (F_δ) are considered as the inputs to the EPS system:

$$u_{EPS}(t) = \begin{bmatrix} u & T_d & F_{\cdot} \end{bmatrix}^T$$

The output $y(t)$ of the EPS system is the column torque T_{col}:

$$y(t) = T_{col} = \frac{1}{C_{21}} q_{21} \tag{11}$$

The system matrices A, B and C are given as:

$$A = \begin{bmatrix} -\frac{R_2}{I_3} & -\frac{r_1}{I_7} & 0 & 0 & 0 & 0 & 0 & 0 & 0 \\ \frac{r_1}{I_3} & -\frac{R_6}{I_7} & -\frac{1}{C_9} & 0 & 0 & 0 & 0 & 0 & 0 \\ 0 & \frac{1}{I_7} & 0 & 0 & 0 & -\frac{1}{m_1 I_{18}} & 0 & 0 & 0 \\ 0 & 0 & 0 & -\frac{R_{13}}{I_{14}} & -\frac{1}{C_{16}} & 0 & 0 & 0 & 0 \\ 0 & 0 & 0 & \frac{1}{I_{14}} & 0 & -\frac{1}{I_{18}} & 0 & 0 & 0 \\ 0 & 0 & \frac{1}{m_1 C_9} & 0 & \frac{1}{C_{16}} & -\frac{R_{19}}{I_{18}} & -\frac{1}{C_{21}} & 0 & 0 \\ 0 & 0 & 0 & 0 & 0 & \frac{1}{I_{18}} & 0 & -\frac{1}{m_2 I_{25}} & 0 \\ 0 & 0 & 0 & 0 & 0 & 0 & \frac{1}{m_2 C_{21}} & -\frac{R_{24}}{I_{25}} & -\frac{1}{C_{26}} \\ 0 & 0 & 0 & 0 & 0 & 0 & 0 & \frac{1}{I_{25}} & 0 \end{bmatrix}$$

$$B = \begin{bmatrix} 1 & 0 & 0 & 0 & 0 & 0 & 0 & 0 & 0 \\ 0 & 0 & 0 & 1 & 0 & 0 & 0 & 0 & 0 \\ 0 & 0 & 0 & 0 & 0 & 0 & 0 & 1 & 0 \end{bmatrix}^T$$

$$C = \begin{bmatrix} 0 & 0 & 0 & 0 & 0 & 0 & \frac{1}{C_{21}} & 0 & 0 \end{bmatrix} \tag{12}$$

3. Controller Design

3.1 PID Controller Design of EPS System

Proportional Integral Derivative (PID) controllers with compensators have been extensively and successfully implemented in EPS systems[12-14]. The advantages of compensators and PID control algorithms over other control methods are their simple structure and low implementation cost. A typical PID control strategy of EPS is presented in the block diagram of Figure 3[15].

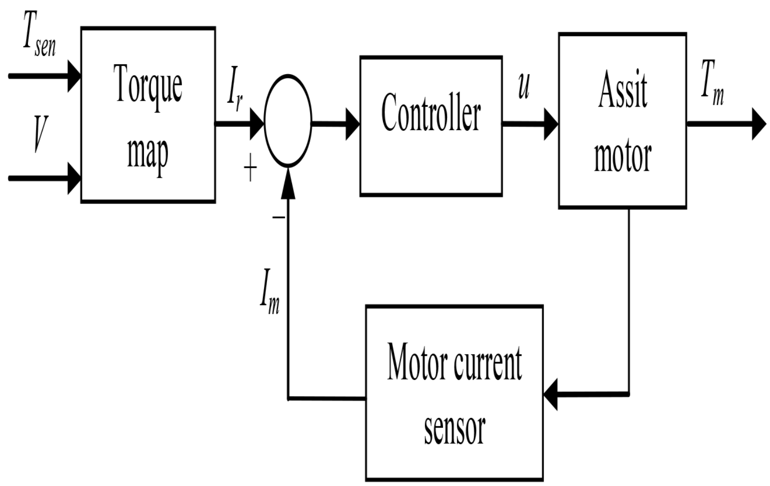

Figure 3. EPS control diagram system.

Where $u(t)$ is the control signal, T_{sen} is the torque sensor, V is the vehicle speed, T_m is the torque motor and $e(t)$ is the error between the desired current motor (I_r) and the current motor I_m of DC motor ($e(t) = I_r - I_m$).

3.2 FTC Controller Design

The controller block diagram is presented in Figure 4. The state-space approach is employed to obtain a suitable controller for the EPS system. It can be shown, that for the state-space model described in equation (10), the pair (A, B) is controllable and the pair (A, C) is observable.

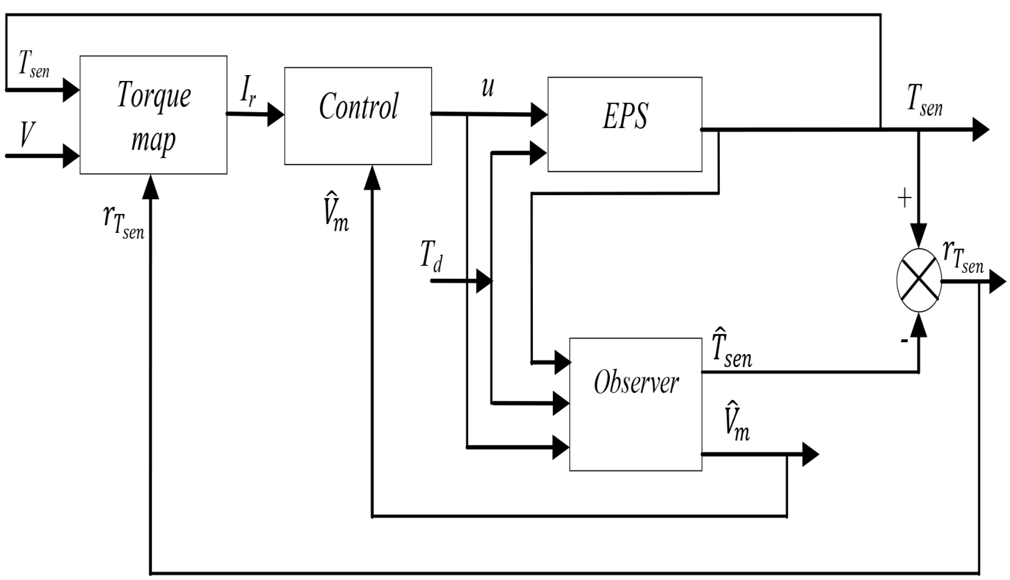

Figure 4. EPS Controller block diagram.

Where Tsen is the torque sensor, $\hat{V}_m$ is the velocity of DC motor estimated by Luenberger observer, $r_{T_{sen}}$ is the residual of torque sensor, $\check{T}_{sen}$ is the torque sensor also estimated by Luenberger observer, V is the vehicle speed signal, I_{des} is the desired current of motor, u is the output of control block and also is the input voltage of DC motor and T_d is the input driver torque.

3.2.1 Diagnosis Block Diagram

To investigate the application of control to the EPS systems, a Luenberger observer based fault tolerant controller is presented. For the dynamical system given by (10), a Luenberger observer is designed and the state equation becomes:

$$\begin{cases} \dot{\hat{x}}(t) = A\hat{x}(t) + Bu^{EPS}(t) + L\left(y(t) - C\hat{x}(t)\right) \\ y(t) = C\hat{x}(t) \end{cases} \tag{14}$$

Where $\hat{x}(t)$ is the estimate of the system state, L is the estimator gain matrix and $\hat{y}(t)$ is the estimated output.

$$L = PC^T R_1^{-1} \tag{15}$$

$$\dot{P} = AP + XA^T - XC^T R_1^{-1} CX + Q_1 \tag{16}$$

Where R_1 is positive definite matrix and Q_1 is a positive, semi-definite matrix and P is the positive definite solution to the Riccati equation[16].

3.2.2 Controller Block Diagram

The main control strategy proposed here is to achieve active torque control by directly control the motor voltage. The control block is needed to produce the assistance motor current to be applied to the steering motor in order to improve the driver's feel. The new control approach which presented in Figure 5 is based on inverse BG model of DC motor.

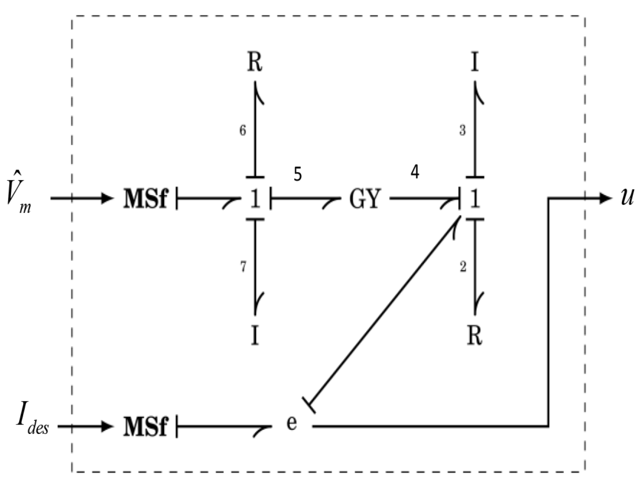

Figure 5. Control block based inverse BG model of DC motor.

In Figure 5, they are tow reference input of DC motor: desired current (I_r) and estimated velocity ($\hat{V}_m$) of DC motor provided by the Luenberger observer. So, the control input signal (u) of DC motor is given by equation (17).

$$u = \left(N_x\right)^T \begin{bmatrix} \dot{I}_r \\ \dot{\hat{V}}_m \end{bmatrix} + \left(N_u\right)^T \begin{bmatrix} I_r \\ \hat{V}_m \end{bmatrix} \tag{17}$$

Where N_u and N_x are matrix gain to be computed. I_r is the desired current of motor based on the torque map is determined by equation (27) and $\hat{V}_m$ is the velocity of DC motor is estimated by the Luenberger observer.

3.2.3 Compute the N_u Matrix and N_x

Consider the reference system shown by equation (18). N_u and N_x are calculates such that y_r(t) is equal to reference input r(t)[17].

$$\begin{cases} \dot{x}_r(t) = A_m x_r(t) + B_m u_r(t) \\ y_r(t) = C_m x_r(t) \end{cases} \tag{18}$$

The basic idea to find the gain N_x that it should transform the reference input r(t) to a state reference x_r(t).

$$x_r(t) = N_x y_r(t) \tag{19}$$

Additionally, in order to remove the steady state error, a feed-forward control that is proportional to the reference input is added

$$u_r(t) = N_u r(t) \tag{20}$$

where N_x and N_u can be designed as follows:

$$\begin{cases} N_x \dot{r} = A_m N_x r + B_m N_u r \\ r = C_m N_x r \end{cases} \tag{21}$$

$$\begin{bmatrix} 0 \\ I \end{bmatrix} = \begin{bmatrix} A_m - I & B_m \\ C_m & 0 \end{bmatrix} \begin{bmatrix} N_x \\ N_u \end{bmatrix} \tag{22}$$

So N_x and N_u are calculated by equation (23):

$$\begin{bmatrix} N_x \\ N_u \end{bmatrix} = \begin{bmatrix} A_m - I & B_m \\ C_m & 0 \end{bmatrix}^{-1} \begin{bmatrix} 0 \\ I \end{bmatrix} \tag{23}$$

Where A_m, B_m and C_m are matrices of DC motor are given as:

$$A_m = \begin{bmatrix} -\dfrac{R_2}{I_3} & -\dfrac{r_1}{I_3} \\ \dfrac{r_1}{I_7} & -\dfrac{R_6}{I_7} \end{bmatrix}, \quad B_m = \begin{bmatrix} 1 \\ 0 \end{bmatrix}, \quad C_m = \begin{bmatrix} \dfrac{1}{I_3} & 0 \\ 0 & \dfrac{1}{I_7} \end{bmatrix}$$

Based in the equation (23), the matrix N_x and N_u are calculated by the new equation (24):

$$\begin{bmatrix} N_x \\ N_u \end{bmatrix} = \begin{bmatrix} A_m - I & B_m & 0 \\ C_m & 0 & \beta \end{bmatrix}^{-1} \begin{bmatrix} 0 \\ I_1 \end{bmatrix} \qquad (24)$$

where

$$I_1 = \begin{bmatrix} 1 \\ 0 \end{bmatrix} \text{ and } \beta = \begin{bmatrix} 0 \\ -1 \end{bmatrix}$$

3.2.4 Compute the Desired Current (I_{des})

In nominal condition, the desired current (I_{des}) of DC motor is determined by the equation (25):

$$I_{des} = G.T_{sen} \qquad (25)$$

Where G is constant parameter determined by the assistance law of EPS system presented in Figure 6 and the torque sensor *(T_{sen})* is determined bythe equation (26):

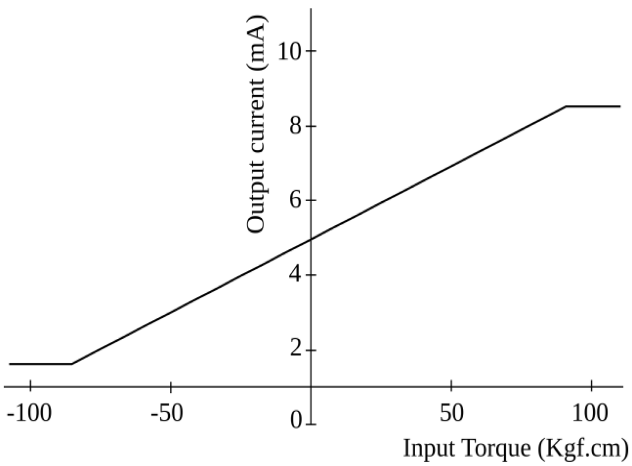

Figure 6. Assistance laws.

$$T_{sen} = T_{sen_0} + \frac{1}{C_{16}} T_d \qquad (26)$$

Where $T_{sen_0} = 5\,mA$ in the initial condition *($T_d = 0$ Nm)* and C_{16} is compliance of torsion bar K_s^{-1}.

Now, when the sensor fault is appeared in the instant t = 5s, so the new desired current motor *(I_{des})* is determined by equation (27):

$$I_{des} = G.(T_{sen} - r_{T_{sen}}) \qquad (27)$$

Where is the residual signal ($r_{T_{sen}} = (T_{sen} - \hat{T}_{sen})$).

4. Results Discussion

To improve the steering feel and maneuverability when the vehicle is turning, a FTC with sensor fault is designed based on the bond graph model. All the simulations have been performed using the software 20sim[18]. The parameters values of EPS system are listed in Table 2.

Table 2. EPS system parameter values

Parameter	Value
R_2	*0.218 Ω*
I_3	*0.710^{-3} H*
r_1	*0.032 Nm/A*
R_6	*3.410^{-4} N/(m/s)*
I_7	*4.810^{-4} Kg m^2*
C_9	*1.5910^{-4} Nm rad/s*
m_1	*0.0434*
I_{13}	*0.0001 Kg m^2*
R_{14}	*0.001 Nm s/rad*
C_{16}	*0.00108 rad/(Nm)*
I_{18}	*0.00149 Kg*
R_{19}	*0.005 Nm s/rad*
C_{21}	*0.110^{-4} Nm rad/s*
m_2	*0.1*
R_{24}	*400 Nm s/rad*
I_{25}	*1 Kg*
C_{26}	*100 rad/Nm*

The speed of the vehicle is set at 2.45 km/h, which is the normal speed in practice as well. Test data is as shown as follows:

The values result of control gains matrix N_x and N_u are:

$$(N_x)^T = [0.0007 \quad 0]$$

$$(N_u)^T = [0.2187 \quad 0.032]$$

The driver input torque signals T_d is shown in Figure 7. The electronic power steering system generates torque through the operation of the motor and the reduction gear installed on the column shaft in order to assist steering effort. In normal condition of system, Figure 8 introduced the current error with PID and FTC approach.

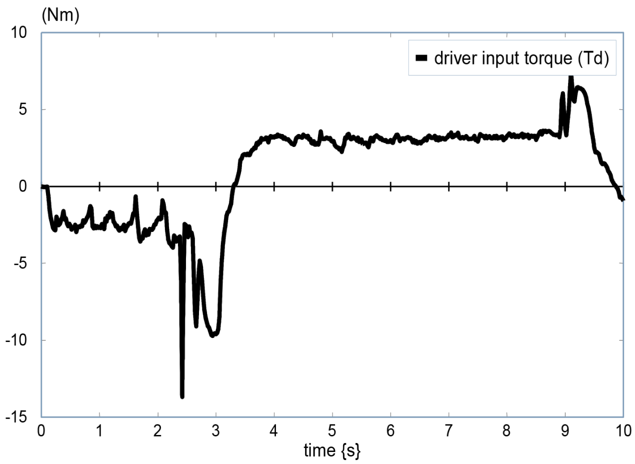

Figure 7. Driver input torque (T_d).

Figure 8, show that the currents error computed with FTC and PID control are not the same. The Figure 8(a) indicates that with PID control, the current error is non-zero. On the other hand, the Figure 8(b) indicates that with FTC, the current of DC motor follows well the desired current.

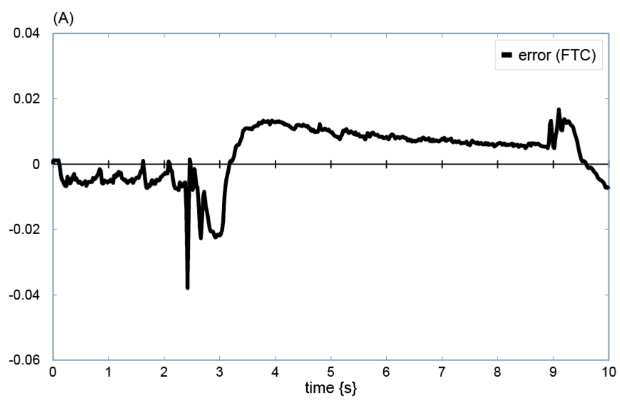

(a)

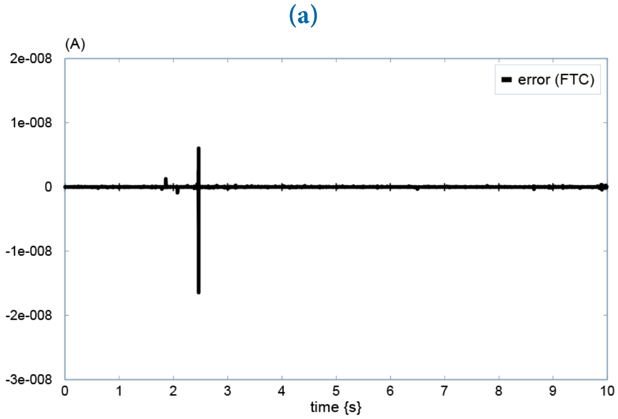

(b)

Figure 8. (a) Current error with PID and (b) current error with FTC in normal condition.

Figure 9 shows that the fault in torque sensor is appeared in instant t = 5s. The residual signal of sensor torque generated by using the Luenberger observer is shown in Figure 10.

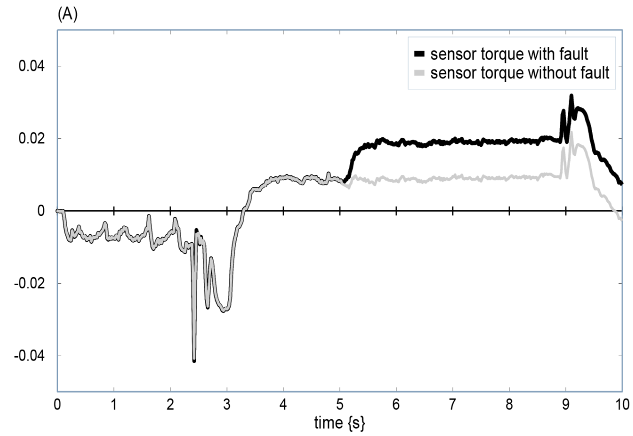

Figure 9 Sensor torque evolution with and without fault.

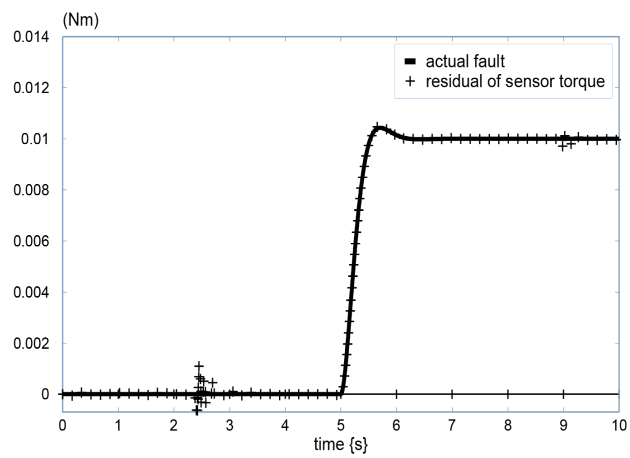

Figure 10. Sensor fault and residual of sensor torque.

Note that the residual signal is equal to actual fault. This residual signal is used in FTC approach to compensate the fault in the system.

In order to show the effective influence of the FTC on the system, a comparative study is proposed between the PID and the proposed FTC controller. Figure 11 shows the result of the motor current evolution in faulty mode.

In presence of sensor fault, the simulation results in Figure 11 indicate that the sensor fault it compensate in motor current value when used the FTC approach. But with PID controller, the motor current value becomes bigger in its amplitudes and indicates the efficiently of the FTC controller method.

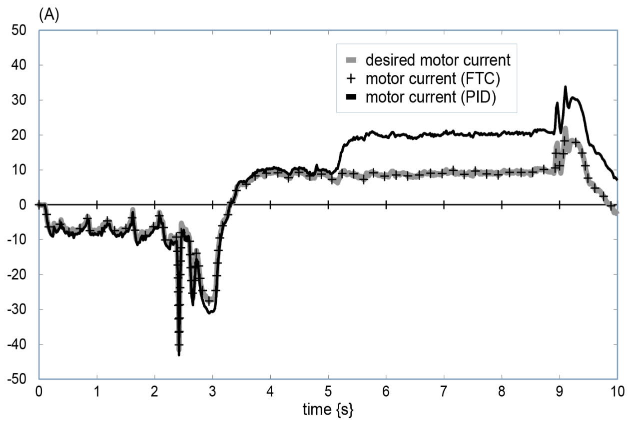

Figure 11. Motor current evolution in faulty condition.

5. Validation Test

This section will present the results obtained from the tests carried on the EPS system in the laboratory presented in Figure 12. The results will be discussed to determine the performance of FTC approach in presence of sensor fault in the EPS system. Figure 13 shows the comparison of simulation results with the experimental results.

Figure 12. EPS experimental test.

Figure 13 show that the simulated results are approximately agreed each other with the real time. The practical results have demonstrated that it is a feasible approach to use a FTC approach that mimics the characteristics of a conventional EPS system in presence of sensor fault.

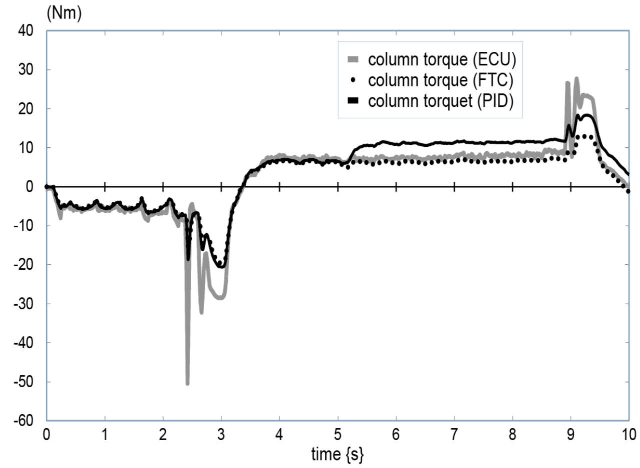

Figure 13. Simulation and experimental test of Column torque.

6. Conclusion

In this paper, we propose an EPS fault tolerant controller system. The novelty of the proposed controller is illustrated by applying the FTC approach based in inverse model of bond graph to the EPS system. Notre approach enables to compute appropriate control actions for compensate the sensor fault. The reconfigurable controller is designed by new algorithm based on Luenberger observer and to compute the controller gain matrix. Simulations have been implemented on EPS system with FTC and PID controller. The fault cannot be eliminated by PID controller, but it is compensated by the FTC approach.

From the experimental results, it is clear that the FTC approach can compensate the fault in the system.

For future work, a more robust observer such as sliding mode observer is recommended to solve the inaccuracy of estimated parameters with presence of sensor fault.

7. References

1. Schoener HP, Hille P. Automotive Power Electronics-New Challenges for Power Electronics. IEEE 31st Annual Power Electronics Specialists Conference. Conference Proceedings (Cat. No.00CH37018). 2000; 1:6-11. Crossref.
2. Lee J, Lee H, Kim J, Jeong J. Model-based fault detection and isolation for electric power steering system. International Conference on Control. Automation and Systems. 2007; p. 2369-74.

3. Izumikawa Y, Yubai K, Hirai J. Fault-Tolerant Control System of Flexible Arm for Sensor Fault by Using Reaction Force Observer. IEEE/ASME Transactions on Mechatronics. 2005; 10(4):391-6. Crossref.
4. Giuseppe S, Menis R, Valla MI. Disturbance Torque Estimation in a Sensorless DC Drive. IEEE Transactions on Industrial Electronics. 1995; 42(4):351-7. Crossref.
5. Edwards C, Tan CP. Fault tolerant control using sliding mode observers. 43rd IEEE Conference on Decision and Control (CDC) (IEEE Cat. No.04CH37601). 2004; 5:5254-9.
6. Campos-Delgado DU, Martinez-Martinez S, Zhou K. Integrated fault-tolerant scheme for a DC speed drive. IEEE/ASME Transactions on Mechatronics. 2005; 10(4):419-27. Crossref.
7. Wang W, Gao Z. A comparison study of advanced state observer design techniques. Proceedings of the American Control Conference. 2003; p. 4754-9. Crossref.
8. Paynter HM. Analysis and design of engineering system. The M.I.T. Press, Boston. 1961. PMid:13733699.
9. Karnopp D. Bond graphs in control: Physical state variables and observers. Journal of the Franklin Institute. 1979; 308(3):221-34. Crossref.
10. Kim JH, Song JB. Control Logic for an Electric Power Steering System Using Assist Motor. Mechatronics. 2002; 12(3):447-59. Crossref.
11. Automotive Engineering. Available from: https://en.wikipedia.org/wiki/Automotive_engineering. Date accessed: 22/05/2018.
12. Wang S, Yin C, Zhao J, Shaohua W, Chunfang Y, Jinbo Z. Design and Full-Vehicle Tests of EPS Control System. International Forum on Computer Science-Technology and Applications. 2009; 2:101-4.
13. Zeng Q, Huang J. The Development of Control Unit in Automotive Electric Power Steering System. Asia-Pacific Conference on Information Processing. 2009; 1:242-5.
14. Chun-Hua H. Modeling and Simulation of Automotive Electric Power Steering System. Second International Symposium on Intelligent Information Technology Application. 2008; 3:436-9.
15. Kim JH, Song JB. Control Logic for an Electric Power Steering System Using Assist Motor. Mechatronics. 2002; 12(3):447-59. Crossref.
16. Willems JC. Least squares stationary optimal control and the algebraic Riccati equation. IEEE Transactions on Automatic Control. 1971; 16(6):621-34. Crossref.
17. Trankle TL, Bryson AE. Control Logic to Track Outputs of a Command Generator. Journal of Guidance, Control, and Dynamics. 1978; 1(2):130-5. Crossref.
18. 20Sim Control lab Products B.V. Available from: http:///www.20sim.com. Date accessed: 01/03/2013.